PERGAMON

Vision Research 40 (2000) 151–162

Vision Research

www.elsevier.com/locate/visres

Unconstrained stereoscopic matching of lines

Raymond van Ee [a,b,*], Clifton M. Schor [a]

[a] *School of Optometry and Vision Science Program, University of California, Berkeley, CA, USA*
[b] *Helmholtz Institute, Utrecht, The Netherlands*

Received 18 February 1999; received in revised form 20 May 1999

Abstract

The computation of horizontal binocular disparities used in stereoscopic depth perception depends upon the identification of corresponding features in the two retinal images. In principle, binocular matching is a two-dimensional problem that considers matches in all possible meridians. Normally, constraints such as end points or crossing points limit the direction and magnitude of matches. If matching is unconstrained, such as is the case with long lines, it is completely ambiguous. Under these conditions the default match will be determined by the operating range, or upper disparity limit, of matchable vertical and horizontal disparities. We computed the operating range of vertical matches for stereoscopic depth as a function of line orientation. Our results suggest that the two-dimensional operating range is anisotropic for vertical and horizontal disparity and that unconstrained matches are not based upon either epipolar geometry or nearest neighbor constraints, but rather the mean of disparity estimates within the operating range for binocular matches. This operating range can be extended vertically when matches are constrained by image primitives. © 2000 Elsevier Science Ltd. All rights reserved.

Keywords: Binocular vision; Stereopsis; Disparity; Matching; Correspondence

1. Introduction

Our retinae receive slightly different two-dimensional (2D) images of objects around us. We retrieve the three-dimensional (3D) lay-out of a scene from the spatial differences between the two retinal images (binocular disparity) (see Howard & Rogers, 1995; Schor, 1999, for recent reviews). The computation of disparities depends upon the correct identification of corresponding features of the two retinal images (e.g. Julesz, 1971). This identification process is commonly referred to as the *matching problem* and the corresponding features are called *matching primitives*. Most natural images contain unambiguous matching primitives. Matching becomes ambiguous when images contain either too many matching candidates or regions that have no primitives. Tree foliage is an example of excessive primitives. Long oblique line stimuli are examples of a void of primitives.

1.1. Line stimuli and availability of matching primitives

The identification of corresponding points is relatively straightforward when there are small isolated features in the visual field, such as shown in Fig. 1A. The matching process for short lines is also straightforward when the endpoints of the line are visible (see Fig. 1B). We will refer to this matching constraint as *endpoint match*. Either the endpoints of the line or the lines as a whole could be regarded as features that disambiguate the matching problem[1]. After matching the endpoints, the intermediate point matches are based on interpolation (Mitchison & McKee, 1985; McKee & Mitchison, 1988; Mitchison, 1988).

The matching process for long oblique lines is highly ambiguous (Ogle, 1950, Chapter 19; Ebenholtz & Walchli, 1965; Blake, Camisa & Antoinetti, 1976;

* Corresponding author. Present address: Department of Brain and Cognitive Sciences, MIT, 79 Amherst Street (E10-120), Cambridge, MA 02139, USA. Fax: +1-617-2538335.
E-mail address: raymond@psyche.mit.edu (R. van Ee)

[1] It is worth noting that Anderson (1994) has shown that multiple depth interpretations are available to the visual system when lines have a vertical shift. In some cases the visual system interprets the viewing geometry as being caused by occlusion. In such cases the horizontal shift of the lines is interpreted as horizontal disparity and the endpoints are unmatched.

0042-6989/00/$ - see front matter © 2000 Elsevier Science Ltd. All rights reserved.
PII: S0042-6989(99)00174-1

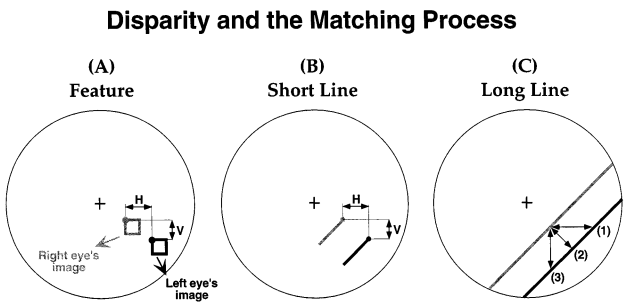

Fig. 1. Schematic explanation of three possible matches of the left retinal image with the disparate right retinal image for three different stimuli. The circle represents the unfused binocular image. The right eye's images are depicted in gray and the left eye's images in black. The cross represents the fixation location (but does not need to be visible). (A) Distinct parts of a feature define matching primitives. For instance the top left corners of the disparate squares are matching primitives. They define horizontal (H) and vertical (V) disparity. (B) The endpoints of the disparate line are matching primitives which can guide stereoscopic matching. (C) For an infinitely long line there are at least three ways of matching. (1) Horizontal; (2) nearest neighbor and (3) vertical. We are dealing with an aperture problem in this situation.

Arditi, Kaufman & Movshon, 1981; Arditi, 1982; Remole, Code, Matyas, McLeod & To, 1992; Morgan & Castet, 1997; Farell, 1998). There are no features that can guide the matching process if the retinal projections of the line are so eccentric that the peripheral visibility is insufficient to define a disparity between the endpoints of the lines. We will refer to such lines as *infinitely* long lines and we will refer to the matching process as being *unconstrained*[2]. In fact we are dealing with a *stereoscopic aperture problem* in the case of such unconstrained matching (Morgan & Castet, 1997). There are an infinite number of possible matches of an infinitely long line in the left eye with a disparate retinal image of the line in the right eye. We have considered three possible matching strategies that have been modeled previously. They are depicted in Fig. 1C and are termed *horizontal match*, *nearest neighbor match* and *vertical match* (e.g. Arditi, 1982; Howard & Rogers, 1995). The exclusive horizontal match, otherwise known as the epipolar constraint (Prazdny, 1983; Faugeras, 1993), gives horizontal disparity the highest weight of all disparity meridians. According to the nearest neighbor constraint, matching is orthogonal to the line (Arditi et al., 1981; Arditi, 1982). The vertical constraint gives vertical disparity the highest weight of all disparity meridians. It is presented to illustrate the role of endpoint matches.

1.2. Aim of this paper

Matching studies in the literature have only addressed matching in the presence of constraining features (such as endpoints or crossings) that could guide the matching process. Little has been studied about matching in unconstrained conditions. Unconstrained conditions do not often occur under daily circumstances. However, matching in ambiguous unconstrained cases (such as the infinite line aperture problem when there is not a single cue to constrain the direction of matching) informs us about the default match.

2. General methods

Consider one infinitely long diagonal line displayed on a screen by means of an anaglyphic stereogram in an otherwise dark room. Suppose that there is a certain horizontal disparity (a horizontal shift on the screen) between the line's stereogram half-images. The magnitude of the sensed or *effective horizontal disparity* will depend upon the meridian of the match. If the visual system's default match is in the horizontal meridian, then the effective horizontal disparity will equal the horizontal offset of the stimulus. However if the default match is in any other meridian (e.g. the nearest neighbor), the horizontal component of this match will be less than the horizontal offset of the stimulus. If we assume that the perceived depth magnitude is solely dependent on the effective horizontal disparity component of a match in any meridian, then the effective horizontal disparity can be estimated with a small depth probe that has well defined matching primitives for vertical and horizontal meridians.

Throughout this paper, we will use such a *depth probe* method (Mitchison & McKee, 1985) to systematically explore the horizontal disparity that is consistent with the line's perceived depth. We will make use of the method of constant stimuli to determine the horizontal disparity between the probe's stereogram half-images that is needed to perceive it at the same depth as the line. The probe location in the right eye's half-image remains the same and its location in the left eye's half-image varies along a virtual oblique path that is parallel to the line (see Fig. 2). When vertical disparity is set to zero, the horizontal separation between the left and right probe images equals the horizontal separation between the left and right images of the line. The horizontal disparity and the corresponding perceived

[2] Unconstrained conditions arise when an image variable can be varying along one spatial dimension without having an effect upon the image. Situations in which unconstrained conditions arise are often called aperture problems (e.g. Morgan & Castet, 1997). For instance the aperture problem in motion perception arises when the vector component of motion is parallel to the stimulus orientation. If the motion vector is decomposed into a parallel and an orthogonal component to the stimulus orientation, only the orthogonal component can be detected. The aperture problem in motion has been much discussed. The analogous problem in stereoscopic vision has been discussed by Morgan and Castet (1997) and Farell (1998) but little is known about the underlying mechanism of matching.

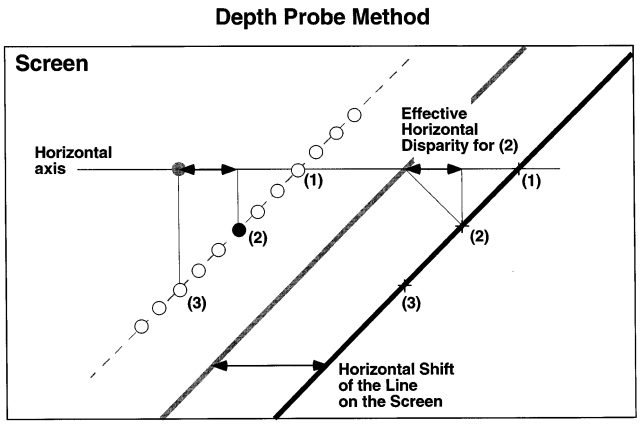

Fig. 2. The depth probe method. We used a depth probe method to systematically explore the perceived depth of a line stimulus. The depth probe is depicted in the left part of the figure and an infinitely long line in the right part of the figure. The right eye's half-image of the line is gray and the left eye's half-image is black. Assume that the visual system's default match of the line is according to the nearest neighbor constraint (2). If this assumption is correct an extra probe in the visual field of which the half-images are shifted according to the nearest neighbor matching constraint (2) must be perceived at the same depth as the line. However, if the default match of the line was horizontally (1), or vertically (3) (or anything except nearest neighbor) then this extra projected probe would be perceived in another depth plane than the depth plane of the line. The right eye's location of the probe (gray dot) remains the same and its left eye's location (open dots) varies along a virtual oblique path (the dashed line) parallel to the line.

depth as well as vertical disparity covary with probe position on the oblique path.

The rationale of the depth probe method is based on the assumption that the horizontal disparity determines the depth between distinct features (see Fig. 2). Indeed from several studies we know that vertical disparity by itself does not alter perceived depth (e.g. Ogle, 1955; Howard & Kaneko, 1994; van Ee & Erkelens, 1995). However the depth induced by horizontal disparity depends on the configuration of vertical disparities in the rest of the visual field (Ogle, 1950; Howard & Rogers, 1995). A depth scaling might take place due to the vertical component of the probe's disparity (Rogers & Bradshaw, 1995). In Experiment 1 we tested the assumption that only the horizontal disparity of the probe determines its perceived depth in our experimental set-up.

After validation of the depth probe method, in the second experiment we investigated how oblique lines (45° with the horizontal) with a range of line lengths are matched. We expected that for short lines, the line's perceived depth is determined by endpoint matching. With increasing line length the matching process should become increasingly ambiguous. In Experiment 3 we investigated default matching of infinitely long oblique lines at various angles with the horizontal.

A target's retinal disparity depends on the torsional state of the eyes and resulting vertical and horizontal disparity components increase with line length. Accordingly, this torsional state is important for interpreting matching results with long lines. Therefore we measured the torsional state of the eyes while subjects binocularly viewed the oblique line stimuli.

2.1. Apparatus

The stimuli were presented dichoptically in the form of stereograms. Observers viewed these stereograms, that were rear-projected onto a large flat screen, at a fixed viewing distance of 150 cm. Every pixel subtended 2.5×2.5 arcmin. The stereograms were presented to the two eyes using the standard red–green anaglyph technique. The intensities of the red and green stereogram half-images were adjusted to appear equally bright when viewed through the red and green filters placed before the eyes. There was no visible crosstalk between the half-images. The room was dark; nothing but the stimulus was visible. The refresh rate of the stimuli was 75 Hz. The head was stabilized with a chin and tightly-fit forehead rest.

2.2. Stimuli

Three different patterns were presented to the subject (see Fig. 3). The grid pattern subtended $41 \times 32°$ in visual angle and every square of the grid subtended $3.6 \times 3.6°$. The grid was used to bring the eyes into

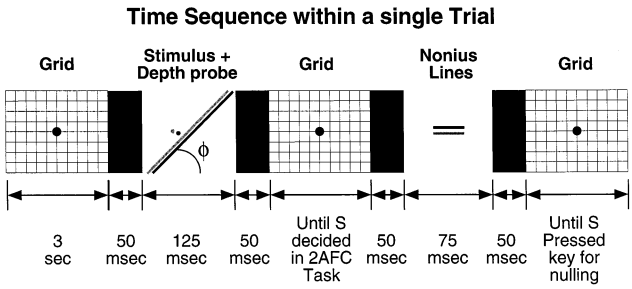

Fig. 3. Time sequence of patterns within a single trial. Every trial started with the presentation of the rectangular grid for 3 s. The grid contained a fixation disk in its center. Then, after a blank time interval of 50 ms the actual stimulus was flashed for 125 ms. This stimulus differed in the various experiments that we conducted. ϕ indicates the slope of the line. Afterwards the grid was visible again until the subject pressed a key to indicate that s/he perceived the probe either in front or behind the line. Then, again after a blank time interval of 50 ms the two nonius lines were flashed simultaneously for 75 ms. Afterwards the grid and the fixation disk were visible again until the subject pressed a key to null the relative rotation between the two nonius lines. The separation between the line, the probe and the fixation disk was always 2.5° (second panel): the depth probe was presented to the left, and below the location of the fixation spot. The nearest point of the line was presented to the right and below the location of the fixation spot.

binocular vertical, horizontal and torsional alignment that remained constant across various stimulus manipulations. The grid contained a fixation disk in the center with a diameter of 40 arcmin. The horizontal and vertical relative disparity of the disk and the grid were zero.

The actual stimulus consisted of the depth probe and the line stimulus. The lines could be presented with variable lengths and slopes. The horizontal shift between the half-images of the infinite line on the screen (the horizontal disparity) was always 15 arcmin (six pixels). The depth probe had a diameter of 15 arcmin. The separation between the line, the depth probe and the fixation disk was always 2.5° (see Fig. 3, second panel from the left). The results of pilot experiments showed that this distance provided optimal circumstances for the present measurements[3].

Flashed (75 ms) horizontal dichoptically presented nonius lines (see Fig. 3) were used to measure the torsional state of the eyes. Briefly flashed stimuli do not influence cyclovergence of the eyes (Sullivan & Kertesz, 1978). The nonius lines had a length of 6° and a vertical separation of 1°. The amount of perceived rotation between the two nonius lines, as measured in a nulling task, indicated the amount of cyclotorsion (Crone & Everhard-Halm, 1975). A nulling procedure was used in which the torsional disparity between the nonius lines was varied until they appeared parallel. This disparity was a measure of the cyclovergence state during stereo tests. This subjective method is preferable to an objective method since an objective method gives relative torsional changes but not absolute measures of binocular cyclovergence.

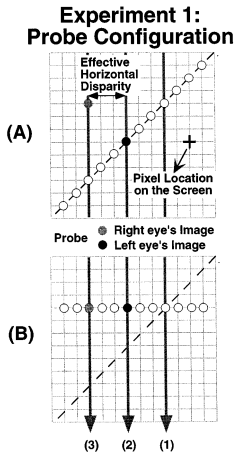

Fig. 4. Experiment 1: validation of the depth probe method. We measured if the probe configurations in (A) or (B) made any difference in the amount of horizontal disparity of the probe that is necessary to perceive it in the same depth plane as the line. The right eye's half-image of the probe (gray disk) was fixed. In condition (A) the location of the left eye's image of the probe (open disks) is chosen from a set of locations along an oblique line which is parallel to the long line. In (A) both the horizontal and vertical disparity of a particular location differed one pixel from their neighbor's location. Every grid intersection can be regarded as a pixel on the screen. In the experiment, the horizontal shift varied between -2 and 9 pixels in the horizontal direction. In (B) the location of the probe's left eye image's is chosen from a set of locations along the horizontal axis. In (B) the probe's vertical disparity is zero and the horizontal disparity of a particular location differed one pixel from their neighbor's location. (1, 2 and 3) represent horizontal, nearest neighbor and vertical match, respectively.

2.3. Task and procedure

We asked subjects to judge whether the depth probe lies in front of, or behind, the line. Before we presented the very first trial in any experimental session, the binocular rectangular grid was shown for 30 s in order to stabilize cyclo, horizontal and vertical vergence. This period of time should be sufficient to stabilize vergence because this period is sufficient to complete a vergence response to considerable torsional as well as vertical and horizontal disparities (Sullivan & Kertesz, 1978). The sequence of stimuli that were presented in a single trial is depicted in Fig. 3. Every trial started with the presentation of the rectangular grid (that also contained the fixation disk (see Fig. 3A) for 3 s. Then, after a blank interval of 50 ms, a line and a probe were flashed simultaneously for 125 ms when the fixation disk was no longer visible. The 125 ms exposure duration is an optimal stimulus for transient stereopsis, which has a larger disparity operating range than the sustained stereo system (Mitchell, 1969; Richards & Kaye, 1974; Pope, Edwards and Schor, 1999). Afterwards, both the grid and fixation disk were again visible until the subject pressed a button to indicate that she/he perceived the probe either in front or behind the line. Then, after another blank time interval of 50 ms, the two nonius lines were flashed simultaneously for 75 ms. We asked subjects to null the relative torsion between the two nonius lines. This was done with repeated flashes of the nonius lines interleaved with the grid.

There were 12 different probe configurations per condition. The locations of both the left and right half-images of the probe are depicted in Fig. 4A. Both the horizontal and vertical disparity of a particular probe location differed one pixel from their neighbor's location. Every trial was repeated seven times. This means that the subject completed 84 trials in every condition. The trials within a session were presented in random order.

[3] The vertical disparity threshold with various image sizes plays an important role. This threshold has been discussed elsewhere (Mitchell, 1966; Duwaer & van den Brink, 1981; Adams, 1998).

2.4. Observers and data analysis

Three subjects took part in the experiments. The subjects had normal or corrected-to-normal vision. Psychometric (probit) functions were fitted to the data in order to determine the location of the point of subjective equality (known as the 50% point). For two subjects the standard deviation in the 50% point across trials was determined by repeating the experiment three times; for the other subject they were determined by a standard Monte-Carlo simulation.

3. Experiment 1: validating the depth probe method

The rationale of the depth probe method is based on the assumption that the horizontal disparity determines the depth between distinct features. As noted above, depth scaling might take place due to the vertical component of the probe's disparity. In Experiment 1 we tested the basic assumption that only the horizontal disparity component of the probe determines its perceived depth.

The methods of Experiment 1 were identical to those described in Section 2. The basic stimulus is presented in Fig. 2. The oblique line was 46° long (which can be considered as infinitely long) and at an angle of 45° to the horizon. The half-images of the depth probe were presented in two configurations (see Fig. 4). The right eye's half-image was fixed in both configurations. In one configuration the location of the probe's left eye's image was chosen from a set of locations along an oblique path parallel to the long line. In the other configuration the location of the probe's left eye's image was chosen from a set of locations along a horizontal path having zero vertical disparity. Thus, both methods adjusted horizontal disparities on the screen. We tested whether the vertical disparities that differed in the two probe configurations influenced the perceived depths stimulated by the horizontal disparity component. Because there were two probe configurations, there were 168 (2×84) trials presented in random order.

3.1. Results

The mean results of the three subjects in Experiment 1 are summarized in Fig. 5, in the same format as we will use for the other graphs. The ordinate shows the horizontal disparity of the probe that is needed to perceive it at the same depth as the diagonal line for the two probe configurations. Along the abscissa, H + V represents the configuration where the probe has horizontal and vertical disparity and H represents the configuration where the probe has horizontal but no vertical disparity. The figure also illustrates predictions for matches for each of the three criteria described earlier. The data lie between predictions of the nearest neighbor and the epipolar constraints. There is no significant ($P < 0.01$) difference between the results obtained with and without the addition of the vertical disparity in the probe. In the rest of the experiments we will use the configuration (H + V) of Fig. 4A where the left eye's probe location varies along a line parallel to the diagonal line.

As noted, we measured how much the eyes were differentially cycloverged while the subjects were performing the experiment. We found that the grid successfully stabilized cyclovergence[4]. The torsional disparities that we found between the nonius lines indicated that the eyes were slightly ex-cycloverged. On average the ex-cyclovergence was $0.4 \pm 0.2°$ across the subjects. This value is in agreement with the results of Nakayama (1983) who measured ex-cyclovergence in primary gaze for various distances. For the viewing distance that we used, interpolation of his data indicates that the ex-cyclovergence was in the order of 0.3°. The ex-cyclovergence values we found were not influenced by the probe configuration. A cyclovergence deviation from zero in the order of 0.4° is insignificant for our experiment given the resolution of our screen because it amounts to a predicted difference of the horizontal disparity on the order of only 0.26 arcmin (and the pixel size is 2.5 arcmin).

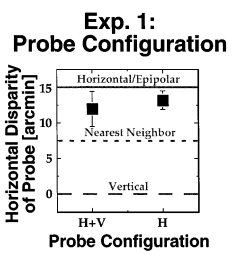

Fig. 5. Results of Experiment 1. The ordinate shows the horizontal disparity of the probe that is needed to perceive it at the same depth as the diagonal line for the two probe configurations. H + V represents configuration (A) in Fig. 4. In condition (A) both the horizontal and vertical disparity of the probe varied. H represents configuration (B) in Fig. 4. In configuration (B) only the horizontal disparity varied. There is no significant ($P < 0.01$) difference between the two conditions. The line had a constant disparity of 15 arcmin. If matching took place along epipolar lines (horizontal lines on the screen) it is predicted that the probe contains 15 arcmin horizontal disparity in order to perceive it at the same depth as the line. The predictions according to the nearest neighbor and vertical matching are shown as well. The error bars represent one standard deviation in the mean across three subjects.

[4] In a control experiment we presented the nonius lines also vertically. The vertical length was 8.5° and the horizontal separation was 2°. This method also revealed that cyclovergence was stabilized across the different presented flashed line stimuli.

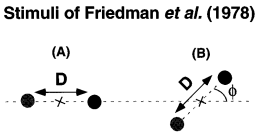

Fig. 6. Stimuli used by Friedman et al. (1978). Subjects estimated the depth of the disparate dot. The black and gray disk represents the left and right half-image of the dot, respectively. The orientation of the dots relative to horizontal (ϕ) was the interesting variable in their experiment. The two half-images of the dot were shifted by a fixed distance of 1°. The diameter of the dot was 15 arcmin. Fixation was on the cross between the half-images of the dot.

3.2. Discussion

Friedman, Kaye and Richards (1978) conducted a similar experiment. They used one dot instead of a line and a probe, and a metrical depth estimation of the dot instead of judging relative depth. When the subject indicated that she/he was fixating a cross between the locations of the dot in the two half-images (see Fig. 6), the experimenter flashed on the two half-images of the dot. The subject then estimated the depth of the flashed dot as a percentage of the distance to the screen. The half-images of the dot had a fixed separation of 1° as the axis of the two half-images was oriented at various angles ϕ (see Fig. 6). Thus, for an orientation of 0°, the horizontal disparity was 1° and the vertical disparity was 0. For an orientation of 90°, the horizontal disparity was 0 and the vertical disparity was 1°. The authors reported that vertical disparity leads to an attenuation of the effect of horizontal disparity. In our study the difference between the conditions H + V and H was not significant ($P < 0.01$). Friedman et al. did not report standard deviations so we don't know how significant their results were.

4. Experiment 2: different line lengths

In the second experiment we examined the matching process for different line lengths. There were four different line lengths: 0.4; 4; 20 and 46° illustrated in Fig. 7. For short lines we predicted that matching will be according to the direction of the shift of the endpoints between the two half-images. That is, according to feature matching. If the half-images of short lines are shifted vertically we predicted that the half-images of the depth probe will have to be shifted vertically for it to be perceived in the same depth plane as the line. The right panel of Fig. 8 shows the predictions in this experiment based on both feature matching and epipolar matching.

For every line length there were three conditions: horizontal shift, vertical shift and perpendicular shift between the half-images of the lines. For the infinitely long line, these three shifts lead to exactly the same

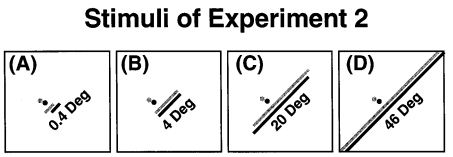

Fig. 7. Stimulus of Experiment 2. In this experiment there were 12 different conditions: four line lengths × three ways of shifting the lines relative to each other. Four characteristic conditions are depicted. In panel (A) the half-images of a line with length 0.4° are shifted horizontally. Endpoint matching predicts that the half-images of the depth probe have to be shifted horizontally in order to perceive the probe at the same depth as the line. In panel (B) the shift is perpendicular to the line, which has now a length of 4°. Endpoint matching predicts that the half-images of the depth probe have to be shifted in a nearest neighbor fashion in order to perceive the probe in the same depth plane as the line. In panel (C) the half-images of the line (20°) are shifted vertically. For an infinitely (46°) long diagonal line (D) it does not matter how the half-images are shifted because the endpoints of the line are not visible.

configuration on the screen because the endpoints are invisible and the horizontal disparity is identical in the three configurations. In the case of the perpendicular shifts, the half-images were translated perpendicular to the slope of the line. The depth probe was adjusted along the diagonal path that was parallel to the line stimulus, as in Experiment 1.

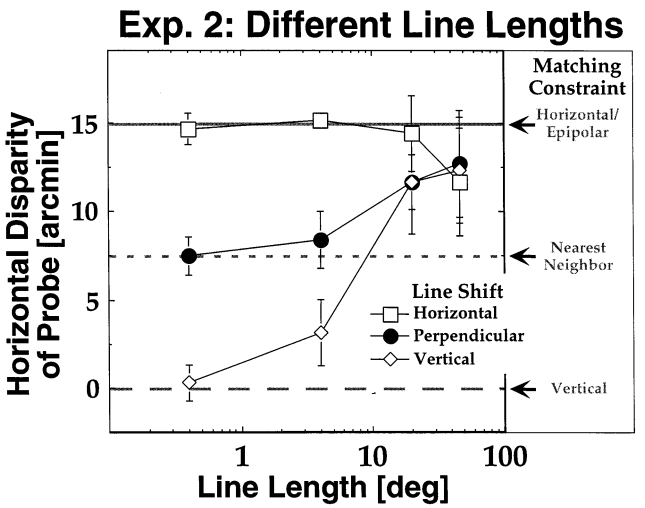

Fig. 8. Results of Experiment 2. The ordinate shows the horizontal disparity of the probe that is needed to perceive it at the same depth as the diagonal line. □, ● and ◇ represent horizontal, perpendicular and vertical shift of the lines, respectively. The right panel shows three matching constraints; these predictions are based on endpoint matching. The gray top line represents horizontal matching which is identical to epipolar matching in our experimental set-up. The probe disparity is then identical to the horizontal shift of the line (which is fixed to 15 arcmin). The gray line in the middle represents nearest neighbor matching. The horizontal shift of points that are matched in this fashion is 7.5 arcmin when the line has a slope of 45°. The gray bottom line represents vertical matching. The horizontal shift is then 0 arcmin. For short lines matching is according to end point matching. The default match for long lines is in between nearest neighbor and horizontal matching. The error bars represent one standard deviation in the mean across three subjects.

In summary, in Experiment 2 there were 252 (3×84) trials for each of the four line lengths. For every line length we devoted a separate experimental session in which the trials were presented in random order.

4.1. Results

The mean results of the three subjects are summarized in Fig. 8. The ordinate indicates the horizontal disparity of the probe that is needed to perceive it at the same depth as the diagonal line element. The abscissa represents the line length.

For short lines, matching follows the end point constraint. If the half-images of a short line element are shifted vertically (the left most diamond in Fig. 8), corresponding to zero horizontal disparity, then the horizontal disparity of the probe that is needed to perceive it at the same depth as the short line element is also zero. If the half-images of a short line element are shifted horizontally (the left most square in Fig. 8), corresponding to horizontal disparity of 15 arcmin, then the horizontal disparity of the probe that is needed to perceive it at the same depth as the short line element is 15 arcmin.

The longer the line, the more matching approaches a value in between epipolar and nearest neighbor constraints. For a long line the same disparity is produced if the half-images are shifted horizontally, vertically or diagonally; the stimulus that is presented to the subject is the same because the endpoints fall outside the screen. The long-line result reveals the direction of the default match for unconstrained stimuli. Note that the result for the long line replicates the result of Experiment 1. The results of the torsion control experiment were also similar to the results reported in Experiment 1. The different line lengths had no influence on the stabilization of torsion and the ex-cyclovergence was 0.3° in this experiment.

4.2. Discussion

Arditi (1982) studied the perceived depth evoked by patterns of oblique lines that were vertically magnified in one eye's half-image. The lines had a length of 6.9° and the endpoints were visible. He suggested that stereoscopic acuity and apparent depth of oblique lines that are vertically magnified in one half-image are determined by the horizontal separation between binocular points which are nearest in a fixed binocular coordinate map, (nearest neighbor constraint) rather than by purely horizontal point-matching (epipolar constraint). Our results in Fig. 8 suggest that binocular matches for lines of 6.9° are based on the endpoint constraint rather than the nearest neighbor constraint. There are clear differences between the stimuli used in his and our study. Arditi presented line patterns that were vertically magnified in one of the two half-images, and we presented a single line that was vertically shifted in the two half-images. Moreover, Arditi did not conduct a matching experiment because the vertical disparities in his stimulus evoked a surface that was slanted in depth. Arditi's study illustrates the influence of line orientation on perceived slant from vertically scaled patterns, however it does not provide information about binocular matching criteria.

5. Experiment 3: various line angles

In Experiment 3 we measured default matching for long oblique lines at different angles to the horizon. The slopes were 20, 35, 45, 65 and 90°. Theoretically, it is impossible to make use of the epipolar constraint in the matching process for long horizontal lines whose endpoints are not visible. Therefore we expect that the visual system would have greater difficulty matching lines oriented at 20° than those at 65° since stereoscopic thresholds increase with decreasing line slopes (see also Ebenholtz & Walchli, 1965; Blake et al., 1976; Howard & Rogers, 1995).

We devoted a separate experimental session for every line angle. There were five sessions, each containing 84 randomly presented trials. In these experiments, the depth probe was adjusted along a diagonal path that was parallel to the test line, as in Experiments 1 and 2.

5.1. Results

Fig. 9A shows the horizontal disparity of the probe that is needed to perceive it at the same depth as the line as a function of line angle. The filled and open squares in Fig. 9A represent the data of two subjects; as opposed to the other two experiments, we did not average the results of the two subjects because this would mask the large error bars within the individual subject-data for the 20° line. Subjects were unable to perform the task for the line with a slope less than roughly 30°. The results of the cyclovergence control experiment were similar to the results reported in Experiments 1 and 2. The different angles of the flashed line had no influence on the stabilization of torsion and the ex-cyclovergence was again 0.3°.

The results at 45° replicate the results from Experiments 1 and 2. For the lines with slopes of 65 and 90°, the default match was somewhat different from horizontal (or epipolar) matching: the horizontal disparity of the probe that was needed to perceive it at the same depth as the vertical line was somewhat smaller than the horizontal disparity of the line. The difference is less than one pixel in disparity but it is consistent. Indeed, observers experienced in psychophysics noted that the probe looked somewhat nearer than the line, even when

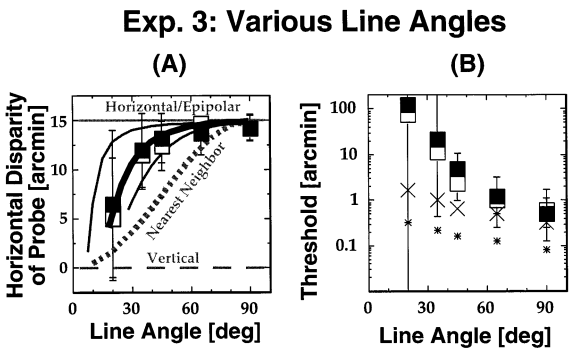

Fig. 9. Results of two subjects in Experiment 3. ■ and □ show the results of subject JZE and SNP, respectively. Panel A portrays the horizontal disparity of the probe that is needed to perceive it at the same depth as the diagonal line. Panel B portrays the thresholds calculated from the slopes in the psychometric functions of the two subjects (see text for details). The crosses in panel B represent Ebenholtz and Walchli's (1965) data, the star symbols represent Blake et al.'s (1978) data. Subjects were practically unable to perform the task at orientations smaller than 30°. The error bars represent one standard deviation determined by a Monte Carlo simulation. The prediction for a direction(vector)-average matching model in (A) is determined by the line angle (ϕ_l) and the horizontal shift (δ_h) on the screen: $\delta_h \cdot \sin^2(\phi_l)$ (dashed thick gray line). The black line in (A) represents a fit in which the vertical operating range V_R is equal to 10 arcmin. The upper curved gray line in (A) is determined by V_R equal to 8 arcmin. The lower curved gray line is determined by V_R is equal to 16 arcmin (see Section 6 for more details).

they both had the same horizontal disparity. The dot's diameter (15 arcmin) was considerably larger than the width of the line (5 arcmin). This diameter was necessary to make the probe sufficiently visible in the conditions in which the task was considered as very difficult by the observers. This monocular size effect could explain the difference between the default horizontal matches for vertical and 65° oblique lines. This effect is presumably constant over the different conditions. (The gray curved lines around the data in Fig. 9A are determined by fits according to a model that we will present in Section 6.)

5.2. Discussion

Both Ebenholtz and Walchli (1965) and Blake et al. (1976) performed similar studies but they were interested in determining the threshold of depth discrimination (as opposed to bias that was our primary interest). Both groups found that stereoscopic threshold depends on the slope of the line. Their data are shown in Fig. 9B together with the thresholds extracted from our data[5]. Our data differ dramatically from theirs for lines with an orientation smaller than 45°. Our subjects had higher thresholds than theirs. In fact, our subjects were not able to perform the depth judgment task for line angles smaller than about 30°. There are however clear differences between our experimental paradigms that could account for these differences. Both previous studies used short lines ($< 2°$) that were physically behind an aperture (whereas we did not use an aperture). They also used thin (1.4 arcmin wide) real lines, whereas we used computer generated thick lines (5 arcmin wide). Another critical difference is the presentation period that was either 10 s (Ebenholtz & Walchli, 1965) or unlimited (Blake et al., 1976). In our study it was only 125 ms because we wanted to prevent eye movements. In their studies, eye movements were not controlled.

[5] Thresholds were defined in terms of the differences between disparities, associated with response probabilities of 50 and 75%, respectively in the method of constant stimuli (our data, Ebenholtz & Walchli, 1965) or as standard deviation in a staircase method (Blake et al. 1976).

6. General discussion

The computation of disparities depends upon the correct identification of corresponding features in the two retinal images. Physiologically, all meridians, or directions, of disparity are coded; in principle, binocular matching is a two-dimensional problem that considers matches in all possible meridians (Morgan & Castet, 1997; Stevenson & Schor, 1997; Farell, 1998). Normally, constraining primitives bias matches and limit the direction of matches: when features, such as the end points of a line, are clearly visible in the two eyes, stereoscopic matches are biased in the direction of the primitives (our Experiment 2).

If matching is unconstrained, such as is the case with long lines, the direction of matches is completely ambiguous. Under these conditions the visual system could select a solution from the entire range of possible ambiguous matches within the usable range from some measure of central tendency. The default match would be determined by the operating range of matchable horizontal and vertical disparities. This operating range could be regarded as being analogous to the 2D disparity range of Panum's area for fusion.

If there is an extreme orientation anisotropy in the operating range for vertical and horizontal disparity, with the vertical range close to zero, then epipolar matching should be the solution in ambiguous conditions (Fig. 10A). If all horizontal and vertical disparities have equal representation, matches in ambiguous cases would follow the nearest neighbor solution, consistent with matches made perpendicular to the line orientation (illustrated in Fig. 10B).

In the case of an anisotropic operating range of matchable disparities, in which the horizontal component has a greater range than the vertical component, matches will fall between these two extreme cases. The bias would approach the nearest neighbor direction for line orientations that deviate from vertical (Fig. 11).

This is illustrated in Fig. 11B. This behavior is consistent with our findings in Experiment 3: first, the default match is consistently between the epipolar/horizontal and the nearest neighbor match and secondly, subjects find it increasingly difficult to match lines when the orientation of the line approaches the horizon.

The direction of matching (α_M) is modeled by the following relationship,

$$\alpha_M = (\beta_1 + \beta_2)/2 \quad (1)$$

where β equals the angular range of disparity vectors that can be coded within the operating range and α_M is the mean of that range. Sensory studies of fusion demonstrate that there is a considerably greater range of horizontal than vertical disparities for the singleness percept (e.g. Mitchell, 1966; Schor & Tyler, 1981; Schor, Wood & Ogawa, 1984; Schor, 1999). Do similar vertical boundaries constrain stereoscopic matching? If so, the size of the vertical range will be the primary constraint on matches within the operating range for binocular matches. We have examined stereoscopic matches as a function of line orientation and we have exploited the fact that the direction of the match determines the magnitude of the effective horizontal disparity component that stimulates stereo depth (see Figs. 2 and 10). Straightforward geometry reveals that the relationship between the matching direction (α_M), the effective horizontal disparity ($\delta_{\text{horizontal, effective}}$) and line angle ($\phi_l$) is given by:

$$\alpha_M = \text{ArcTan}\left[\left(1 - \frac{\delta_{\text{horizontal}}}{\delta_{\text{horizontal, effective}}}\right)\cdot\text{Tan}\ \phi_l\right]. \quad (2)$$

Here $\delta_{\text{horizontal}}$ denotes the disparity of the line that would be produced by a pure horizontal match between dichoptic lines. The $\delta_{\text{horizontal, effective}}$ is the horizontal disparity of the depth probe used to match the perceived depth of the oblique line. From the relationship $\alpha_M = (\beta_1 + \beta_2)/2$ we are able to determine a relationship between the matching direction (α_M), the vertical operating range (V_R), the orientation (ϕ_l) and horizontal disparity ($\delta_{\text{horizontal}}$) of the line:

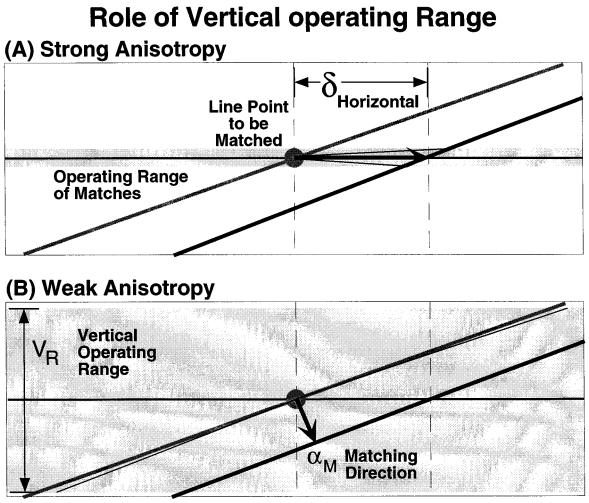

Fig. 10. The role of the vertical operation range of matchable disparities. The default match in unconstrained conditions will be determined by the operating range of matchable vertical disparities (V_R). Panel A illustrates that if there is an extreme directional anisotropy, with matches only made for horizontal disparities, then epipolar matches should be the solution in ambiguous figures. Panel B illustrates when the operating range of vertical disparity is increased, matches would be biased toward the direction perpendicular to the line. That is, toward the nearest neighbor direction. In this figure, the horizontal range is unlimited. If both horizontal and vertical disparities had equal representation, the matching direction for the example in panel B would have been closer to the nearest neighbor solution (i.e. nearly perpendicular to the line). The rectangular shape of the operating range is a schematic representation of the anisotropy between the vertical and horizontal disparity limits of unconstrained matching. Only the vertical limit is shown. The horizontal range is very large for transient stereopsis (at least 4°) (Richards & Kaye, 1974; Schor et al., 1998) and it is assumed to extend over a much larger disparity range than illustrated by the rectangle.

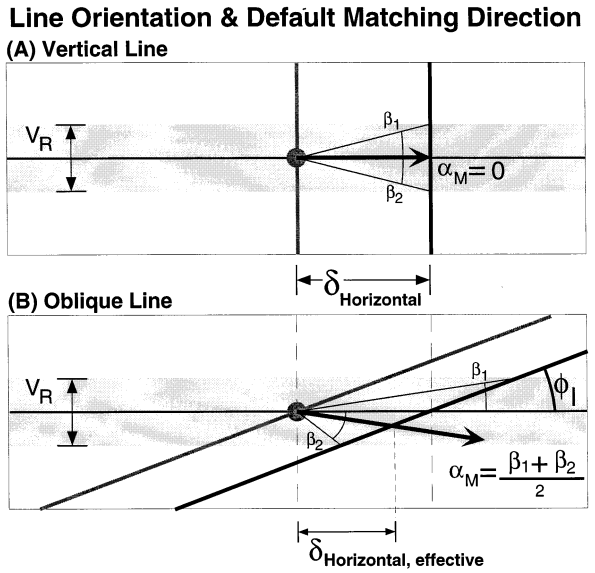

Fig. 11. The role of line orientation on the direction of default matching. The matching direction (α_M) is determined by $(\beta_1 + \beta_2)/2$. The angles β_1 and β_2 are determined by the vertical extent of the anisotropic operating range for binocular matching. In panel A, the target is a vertical line with a horizontal disparity of $\delta_{\text{horizontal}}$. The matching direction is horizontal (epipolar), independent of the vertical operating range (V_R) of matchable disparities. Panel B illustrates that as the line angle decreases, the elongated horizontal operating range biases the matching direction (α_M) away from epipolar toward the nearest neighbor solution (because $\beta_1 < \beta_2$), and the standard deviations in depth discrimination (represented by $\beta_1 + \beta_2$) increase. ϕ_l denotes the target line angle from horizontal. The sensed horizontal disparity that is assigned by the visual system for stereoscopic depth of the line is $\delta_{\text{horizontal, effective}}$. This quantity is smaller than the horizontal stimulus disparity ($\delta_{\text{horizontal}}$).

$$\alpha_M = 0.5\ \mathrm{ArcTan}\left[\frac{V_R}{2\cdot\delta_{horizontal} + V_R\cdot Cot\phi_1}\right] - 0.5\ \mathrm{ArcTan}\left[\frac{V_R}{2\cdot\delta_{horizontal} - V_R\cdot Cot\phi_1}\right] \quad (3)$$

In order to determine the vertical operating range in our Experiment 3, we first established a relationship between the effective horizontal disparity and the line orientation in Eq. (4) for a family of vertical operation ranges by eliminating α_M from Eqs. (2) and (3):

$$\delta_{horizontal,effective} = \frac{\delta_{horizontal}\cdot \mathrm{Tan}\phi_1}{\mathrm{Tan}\phi_1 - \mathrm{Tan}\left[0.5\ \mathrm{ArcTan}\left[\frac{V_R}{2\delta_{horizontal} + V_R\cdot Cot\phi_1}\right] - 0.5\ \mathrm{ArcTan}\left[\frac{V_R}{2\delta_{horizontal} - V_R\cdot Cot\phi_1}\right]\right]} \quad (4)$$

Using a least-squares fit, we solved for the V_R that best fit the data in Fig. 9A. The thick black line in Fig. 9A represents a fit in which the vertical operating range V_R is equal to 10 arcmin ($\pm$ 5 arcmin). The upper gray curved line in Fig. 9A (just above the data) is determined by V_R equal to 8 arcmin. The lower gray curved line (just below the data) is determined by a V_R equal to 16 arcmin. Note that the larger the V_R, the farther the fit deviates from the epipolar match.

The fits based on Eq. (4) become vertical when the line angle decreases (especially for smaller V_R) because it is bounded by a singularity (undefined value) when $\mathrm{Tan}(\Phi_l)$ equals $V_R/2\delta_{horizontal}$. For the horizontal disparity used in this study (15 arcmin) and a V_R of 10 arcmin, a line at an orientation of 18° has an effective horizontal disparity that is undefined. Small variations in line orientation near this value produce very large changes in effective horizontal disparity. Any intrinsic noise for coding this range of orientations would make estimates of effective disparity extremely unreliable. The data in Fig. 9 is consistent with this analysis. This figure shows that the error bars become extremely large in these conditions.

At a line angle near zero the matching direction depends heavily on V_R. Eventually, with very large V_R the horizontal disparity boundary of the operating range would limit the range of effective horizontal disparity. Based upon the measures of upper disparity limits for stereopsis report by Richards and Kaye (1974), this horizontal limit would be about 4° for transient disparity stimuli and based upon the report by Schor et al. (1984) it would be about 1° for static disparity stimuli. Our model predicts an orientation anisotropy for the operating range of vertical and horizontal disparity. The 10 arcmin vertical range is approximately 1/6 the range of horizontal disparity that can be used to process static stereoscopic depth (Schor et al., 1984) and 1/24 of the horizontal disparity range for dynamic stereoscopic depth (Richards and Kaye, 1974).

In Figs. 10 and 11 we represent the operation range by a rectangle. A rectangular operation range does not require an assumption about the horizontal extent of the range. We did not limit the horizontal boundary in order to compute the vertical one. Physiologically, an oval-shaped matching area is probably more plausible than a square-shaped area. The question is, what is the horizontal extent of the oval? For the transient form of stereo that we are studying, it is very large (at least 4° of crossed and uncrossed disparity; see Richards & Kaye, 1974; Schor, Edwards & Pope, 1998). The central component of a very large horizontal ellipse can be approximated by our rectangle. For the range of line orientations that can be matched and for the horizontal disparity that we studied, the current rectangle is sufficiently wide to allow us to estimate the vertical limits of the matching operating range. Our estimate of the operating range for vertical disparity is similar to estimates by Nielsen and Poggio (1984) and Prazdny (1985). This narrow range imposes an effective epipolar constraint that greatly reduces the complexity of two-dimensional binocular matches.

Some tolerance for vertical disparity is necessary to accommodate vertical ocular misalignment, torsional misalignment, geometric perspective distortions of retinal images formed of near objects and anatomical differences in retinal curvature of the two eyes. Small fluctuations of cyclovergence produce cyclo disparities of up to 5 arcmin (Enright, 1990; van Rijn, van der Steen & Collewijn, 1994). Perspective distortion of near targets causes cyclo and vertical disparities of targets above and below the visual plane into the left and right side of fixation (Nakayama, 1983; Gårding, Porrill, Mayhew & Frisby, 1995). At near viewing distances, torsional vergence adjustments during gaze elevation reduce cyclo disparities in the visual plane (retinal equator) (Mok, Ro, Cadera, Crawford & Vilis, 1992; van Rijn & van den Berg, 1993; Tweed, 1997), however cyclo disparities of near targets still remain above and below the point of fixation. There are also naturally occurring errors of vertical eye alignment during normal head movements that introduce vertical disparities (Steinman & Collewijn, 1980). Finally, epipolar planes do not really intersect with constant elevation meridia on the retinae because the center of retinal curvature does not coincide with the nodal point and, second, psychophysical studies indicate that empirical measures of corresponding epipolar lines in the two eyes are not necessarily parallel to one another (Liu & Schor, 1998). These anatomical and optical variations can produce vertical disparity of targets thought to have no physical disparity. Clearly, the limited tolerance for vertical disparity helps compensate for these sources of error.

Other studies have reported operating ranges much larger than 10 arcmin for vertical disparity. All of them

used stimuli with distinct matchable primitives. Ogle (1955) and Mitchell (1970) used isolated line targets and observed transient stereopsis with 4° of added vertical disparity. Stevenson and Schor (1997) used a 12° patch of dynamic random dots and observed transient stereopsis with 45 arcmin of added vertical disparity. Prazdny (1985) and Nielsen and Poggio (1984) also used random dots but found much smaller limits to the useful range of vertical disparity because they used very small patches of random dots (Stevenson & Schor, 1997).

The line stimuli used in the current study are quite large (46°) yet we still observe a small useful range of vertical disparity. In light of prior studies, our results do not specify an absolute limit for vertical disparity processing. Rather, they specify a default range in the absence of matchable primitives. If our results are compared with those of Stevenson and Schor (1997) the vertical disparity operating range can be extended by the presence of matchable primitives by a factor of ten. Binocular receptive fields must have a certain tolerance for vertical disparity that allows for limitations imposed by both imprecision (or noise) in eye posture signals, reduced resolution of disparity detection in the retinal periphery, and imperfections in the retinal shape.

Acknowledgements

R. van Ee was supported by Human Frontier of Science Grant (RG-34/96 to Dr M.S. Banks) and the Foundation for Life Sciences of the Netherlands Organization for Scientific Research (Talent Stipendium, NWO 810-404-006/1 to R. van Ee). C.M. Schor was supported by NIH Grant EYO 8882. We are particularly thankful to Marty Banks and Casper Erkelens who offered inspiring ideas concerning the experimental set-up and interpretation of the results. We are grateful for the help received from Drs W.J. Adams, B.L. Anderson, S.B. Stevenson, and I. Vogels.

References

Adams, W. J. (1998). The role of vertical disparities in human stereo vision. Thesis at University of Sheffield, UK.

Anderson, B. L. (1994). The role of partial occlusion in stereopsis. *Nature*, *367*, 365–368.

Arditi, A. (1982). The dependence of the induced effect on orientation and a hypothesis concerning disparity computations in general. *Vision Research*, *22*, 247–256.

Arditi, A., Kaufman, L., & Movshon, J. A. (1981). A simple explanation of the induced size effect. *Vision Research*, *21*, 755–764.

Blake, R., Camisa, J. M., & Antoinetti, D. N. (1976). Binocular depth discrimination depends on orientation. *Perception and Psychophysics*, *20*, 113–118.

Crone, R. A., & Everhard-Halm, Y. (1975). Optically induced eye torsion. *Albrecht von Graefes Archives of Clinical Experimental Ophthalmology*, *195*, 231–239.

Duwaer, A. L., & van den Brink, G. (1981). What is the diplopia threshold? *Perception and Psychophysics*, *29*, 295–309.

Ebenholtz, S. M., & Walchli, R. (1965). Stereoscopic thresholds as a function of head- and object-orientation. *Vision Research*, *5*, 455–461.

Enright, J. T. (1990). Stereopsis, cyclotorsional noise and the apparent vertical. *Vision Research*, *30*, 1487–1497.

Farell, B. (1998). Two-dimensional matches from one-dimensional stimulus components in human stereopsis. *Nature*, *395*, 689–693.

Faugeras, O. (1993). *Three dimensional computer vision*. Cambridge: MIT.

Friedman, R. B., Kaye, M. G., & Richards, W. (1978). Effect of vertical disparity upon stereoscopic depth. *Vision Research*, *18*, 351–352.

Gårding, J., Porrill, J., Mayhew, J. E., & Frisby, J. P. (1995). Stereopsis, vertical disparity and relief transformations. *Vision Research*, *35*, 703–722.

Howard, I. P., & Kaneko, H. (1994). Relative shear disparities and the perception of surface inclination. *Vision Research*, *34*, 2505–2517.

Howard, I. P., & Rogers, B. J. (1995). *Binocular vision and stereopsis*. New York: Oxford.

Julesz, B. (1971). *Foundations of cyclopean perception*. Chicago: University of Chicago.

Liu, L., & Schor, C. M. (1998). Functional division of the retina and binocular correspondence. *Journal of the Optical Society of America*, *15*, 1740–1755.

McKee, S. P., & Mitchison, G. J. (1988). The role of retinal correspondence in stereoscopic matching. *Vision Research*, *28*, 1001–1012.

Mitchell, D. E. (1966). A review of the concept of Panum's fusional areas. *American Journal of Optometry*, *43*, 387–401.

Mitchell, D. E. (1969). Qualitative depth localization with diplopic images of dissimilar shape. *Vision Research*, *9*, 991–994.

Mitchell, D. E. (1970). Properties of stimuli eliciting vergence eye movements and stereopsis. *Vision Research*, *10*, 145.

Mitchison, G. J. (1988). Planarity and segmentation in stereoscopic matching. *Perception*, *17*, 753–782.

Mitchison, G. J., & McKee, S. P. (1985). Interpolation in stereoscopic matching. *Nature*, *315*, 402–404.

Mok, D., Ro, A., Cadera, W., Crawford, J. D., & Vilis, T (1992). Rotation of Listing's plane during vergence. *Vision Research*, *32*, 2055–2064.

Morgan, M. J., & Castet, E. (1997). The aperture problem in stereopsis. *Vision Research*, *37*, 2737–2744.

Nakayama, K. (1983). Kinematics of normal and strabismic eyes. In C. M. Schor, & K. J. Ciuffreda, *Vergence eye movements: basic and clinical aspects* (pp. 543–564). Boston: Butterworths.

Nielsen, K. R. K., & Poggio, T. (1984). Vertical image registration in stereopsis. *Vision Research*, *24*, 1133–1140.

Ogle, K. N. (1950). *Researches in binocular vision*. London: W.B. Saunders.

Ogle, K. N. (1955). Stereopsis and vertical disparity. *Archives of Ophthalmology*, *53*, 495–504.

Pope, D. R., Edwards, M., & Schor, C. M. (1999). Extraction of depth from opposite-contrast stimuli: transient system can, sustained system can't. *Vision Research*, *39*, 4010–4017.

Prazdny, K. (1983). Stereoscopic matching, eye position, and absolute depth. *Perception*, *12*, 151–160.

Prazdny, K. (1985). Vertical disparity tolerance in random-dot stereograms. *Bulletin of the Psychonomic Society*, *23*, 413–414.

Remole, A., Code, S. M., Matyas, C. E., McLeod, M. A., & To, C. K. (1992). Multimeridional apparent frontoparallel plane: relation between stimulus orientation angle and compensating tilt angle. *Optometry and Vision Science*, *69*, 544–549.

Richards, W, & Kaye, M. G. (1974). Local versus global stereopsis: two mechanisms? *Vision Research*, *14*, 1345–1347.

Rogers, B., & Bradshaw, M. (1995). Disparity scaling and the perception of frontoparallel surfaces. *Perception*, *24*, 155–179.

Schor, C. M., Edwards, M., & Pope, D. R. (1998). Spatial-frequency tuning of the transient-stereopsis system. *Vision Research*, *38*, 3057–3068.

Schor, C. M., & Tyler, C. W. (1981). Spatio-temporal properties of Panum's fusional area. *Vision Research*, *21*, 683–692.

Schor, C. M. (1999). Binocular vision. In K. Devalois, *Seeing: handbook of perception and cognition*. San Francisco: Academic.

Schor, C. M., Wood, I., & Ogawa, C. M. (1984). Binocular sensory fusion is limited by spatial resolution. *Vision Research*, *24*, 661–665.

Steinman, R. M., & Collewijn, H. (1980). Binocular retinal image motion during active head rotation. *Vision Research*, *20*, 415–429.

Stevenson, S. B., & Schor, C. M. (1997). Human stereo matching is not restricted to epipolar lines. *Vision Research*, *37*, 2717–2723.

Sullivan, M. J., & Kertesz, A. E. (1978). Binocular coordination of torsional eye movements in cyclofusional response. *Vision Research*, *18*, 943–949.

Tweed, D. (1997). Visual-motor optimization in binocular control. *Vision Research*, *37*, 1939–1951.

van Ee, R., & Erkelens, C. J. (1995). Binocular perception of slant about oblique axes relative to a visual frame of reference. *Perception*, *24*, 299–314.

van Rijn, L. J., & van den Berg, A. V. (1993). Binocular eye orientation during fixations: Listing's law extended to include eye vergence. *Vision Research*, *33*, 691–708.

van Rijn, L. J., van der Steen, J., & Collewijn, H (1994). Instability of ocular torsion during fixation: cyclovergence is more stable than cycloversion. *Vision Research*, *34*, 1077–1087.